The Hubbard model on the kagome lattice

The Hubbard model on the kagome lattice

B H Bernhard[1], B Canals[2] and C Lacroix[2]

[1] Departamento de Fisica, Universidade do Estado de Santa Catarina, Joinville, SC, Brazil
[2] Laboratoire de Magnétisme Louis Néel, CNRS, Grenoble, France

E-mail: dfi2bhb@joinville.udesc.br

Abstract

In itinerant magnetically frustrated materials it is important to elucidate the effect of the electronic correlation on the band structure and how it evolves as a function of the electronic concentration n. In this work we address this problem by considering the Hubbard model on a kagome lattice with a single orbital per site, treating the local Coulomb repulsion U within the coherent potential approximation. A metal–insulator transition occurs in the half-filled band ($n = 1$) at $U_c = 3.635t$. A nearly flat band, characteristic of frustrated lattices, is present at the top of the band structure. For concentrations $n > 4/3$, the chemical potential may be located in this very narrow band, and one obtains a significant enhancement of the γ coefficient of the specific heat depending on the value of U. This effect can be at the origin of the heavy fermion behaviour observed in LiV_2O_4.

(Some figures in this article are in colour only in the electronic version)

1. Introduction

The intense work on magnetically frustrated materials has mainly concentrated on localized spin systems [1]. The study of itinerant frustrated systems is motivated by the heavy fermion behaviour observed in the transition metal compounds $Y(Sc)Mn_2$ [2] and LiV_2O_4 [3–5], the discovery of superconductivity in cobaltates [6] and in KOs_2O_6 [7], or the metal–insulator transition observed in pyrochlore iridates [8] or molybdates [9]. LiV_2O_4 is a normal spinel, where V atoms form a pyrochlore lattice. It contains 1.5 3d electrons per V atom distributed among three t_{2g} orbitals and exhibits an enhanced specific heat coefficient $\gamma \approx 420$ mJ mol^{-1} K^{-2}.

Previous studies of such systems using the Hubbard model have been performed with the random phase approximation (RPA) [10–12], the fluctuation exchange (FLEX) approximation [13] and quantum Monte Carlo calculations [14].

We consider here the Hubbard model on a kagome lattice with a single orbital per site. The local Coulomb repulsion U is treated within the coherent potential approximation (CPA) [15]. We are mainly concerned with the effect of U and the electron concentration n upon the band structure and thermodynamic properties.

2. Model and approximation

The kagome lattice can be considered as a triangular lattice with three sites per unit cell forming a triangular basis. The Hubbard Hamiltonian is written as

$$\mathcal{H} = \mathcal{H}_t + \mathcal{H}_U = -\sum_{ij\alpha\beta\sigma} t_{ij}^{\alpha\beta} c_{i\alpha\sigma}^{\dagger} c_{j\beta\sigma} + U \sum_{i\alpha} n_{i\alpha\uparrow} n_{i\alpha\downarrow} \tag{1}$$

where i, j denote sites of the underlying triangular lattice (with lattice parameter $a = 1$) and α, β specify the atoms of the triangular basis. For the hopping matrix elements we take

$$t_{ij}^{\alpha\beta} = \begin{cases} t, & \text{if } (i\alpha) \text{ and } (j\beta) \text{ are nearest neighbours} \\ 0, & \text{otherwise.} \end{cases} \tag{2}$$

The Green functions

$$G_{ij\sigma}^{\alpha\beta} = \langle\langle c_{i\alpha\sigma} ; c_{j\beta\sigma}^{\dagger} \rangle\rangle \tag{3}$$

satisfy the equations of motion

$$\omega G_{ij\sigma}^{\alpha\beta} = \delta_{ij}\delta_{\alpha\beta} + \langle\langle [c_{i\alpha\sigma}, \mathcal{H}] ; c_{j\beta\sigma}^{\dagger} \rangle\rangle. \tag{4}$$

The higher-order Green functions generate an infinite chain of equations, which can be decoupled by some truncation approximation. Here we adopt the CPA decoupling [15], which yields an atomic-like expansion

$$G_{ij\sigma}^{\alpha\beta} = g_{i\alpha}^{\sigma} \left\{ \delta_{ij}\delta_{\alpha\beta} - \sum_{k\gamma} t_{ik}^{\alpha\gamma} G_{kj\sigma}^{\gamma\beta} \right\}. \tag{5}$$

The self-consistent renormalized locator is given by

$$g^{\sigma}(\omega) = \frac{\omega - U + U \langle n_{i\alpha\overline{\sigma}} \rangle - \lambda^{\sigma}}{\omega(\omega - U - \lambda^{\sigma}) + U \langle n_{i\alpha\overline{\sigma}} \rangle \lambda^{\sigma}} \tag{6}$$

where

$$\lambda^{\sigma}(\omega) = 1/g^{\sigma} - 1/G_{ii\sigma}^{\alpha\alpha}. \tag{7}$$

Equation (5) can be formally solved by Fourier transformation. In matrix form

$$\mathbf{G}^{\sigma}(\mathbf{q}) = \left[\mathbf{1} - \mathbf{g}^{\sigma} \boldsymbol{\varepsilon}(\mathbf{q}) \right]^{-1} \mathbf{g}^{\sigma} \tag{8}$$

where $\mathbf{g}^{\sigma} = g^{\sigma}(\omega)\mathbf{1}$. For the kagome lattice,

$$\boldsymbol{\varepsilon}(\mathbf{q}) = -2t \begin{pmatrix} 0 & \cos\left(\frac{q_x - q_y\sqrt{3}}{4}\right) & \cos\left(\frac{q_x + q_y\sqrt{3}}{4}\right) \\ \cos\left(\frac{q_x - q_y\sqrt{3}}{4}\right) & 0 & \cos\left(\frac{q_x}{2}\right) \\ \cos\left(\frac{q_x + q_y\sqrt{3}}{4}\right) & \cos\left(\frac{q_x}{2}\right) & 0 \end{pmatrix} \tag{9}$$

and we obtain

$$G_{\sigma}^{\alpha\alpha}(\mathbf{q}) = \frac{g/3}{1 - 2tg} + \frac{2g(1 + tg)/3}{1 + 2tg - 2t^2g^2 + tg^2\varepsilon_0(\mathbf{q})} \tag{10}$$

where $\varepsilon_0(\mathbf{q})$ is the dispersion relation of the triangular lattice.

The lattice Green functions are obtained by integration over $\mathbf{q}$ which can be converted into a single integral in energy

$$G_{ii\sigma}^{\alpha\alpha} = \int \mathrm{d}E \, \rho_0(E) G_{\sigma}^{\alpha\alpha}(E) \tag{11}$$

where $\rho_0(E)$ is the bare density of states (DOS) of the triangular lattice.

2

The chemical potential μ has to be fixed self-consistently for a given electron concentration

$$n = \sum_\sigma \langle n_{i\alpha\sigma} \rangle = 2 \int d\omega \, f(\omega) \rho_{i\alpha}^\sigma(\omega), \tag{12}$$

where $\rho_{i\alpha}^\sigma(\omega)$ is the local DOS of the kagome lattice and $f(\omega)$ is the Fermi function.

The thermodynamic properties can be addressed through the internal energy per site $E = \langle \mathcal{H} \rangle / N$. The gamma coefficient of the specific heat c is given by

$$\gamma(T) = c(T)/T = (dE/dT)/T. \tag{13}$$

Observing that

$$\sum_{i\sigma} c_{i\sigma}^\dagger [c_{i\alpha\sigma}, \mathcal{H}] = 2\mathcal{H} - \mathcal{H}_t \tag{14}$$

and using equation (4), the internal energy can be evaluated by

$$E = \int d\omega \, f(\omega) \omega \rho^\sigma(\omega) - 4t \langle c_{i\alpha\sigma}^\dagger c_{j\beta\sigma} \rangle_{nn} \tag{15}$$

which involves the nearest-neighbour average

$$\left\langle c_{i\sigma}^\dagger c_{j\sigma} \right\rangle_{nn} = \int d\omega \, f(\omega) \rho_{nn}^\sigma(\omega) \tag{16}$$

where

$$\rho_{nn}^\sigma(\omega) = -\frac{1}{\pi} \operatorname{Im} \left(G_{ij\sigma}^{\alpha\beta}(\omega + i\delta) \right)_{nn}. \tag{17}$$

The Green function in the last equation is related to the local Green function through equation (5).

3. Results and discussion

Figure 1 shows the evolution of the band structure with increasing U close to the metal–insulator transition (MIT) at half-filling ($n = 1$). For $U > U_c = 3.635t$ the Hubbard bands are split and the chemical potential μ is located inside the Hubbard gap. Thin lines correspond to the spectral densities $\rho_{nn}^\sigma(\omega)$ defined in equation (17).

Figure 2 illustrates the transfer of spectral weight from the lower to the upper Hubbard band with increasing electron concentration n for fixed $U = 5t$. In the empty band limit, the lower Hubbard band looks like the uncorrelated DOS. In the opposite limit of large n, it is the upper Hubbard band that acquires a similar shape. In the latter case, the chemical potential is located close to the nearly flat band at the top of the DOS. For intermediate values of n and U, the peak in the DOS is broadened.

The MIT can be followed from the curves of the chemical potential as a function of concentration for fixed values of U. For $U > U_c$ these curves of $\mu(T)$ exhibit a jump at exactly $n = 1$, indicating that the weights of the Hubbard bands are correctly evaluated in the CPA.

Figure 3 shows $\gamma(T)$ for fixed values of U and n. Thin lines indicate the integrated entropy. We see that $\gamma(T)$ may be a non-monotonic function of temperature. Figure 4 describes the enhancement of γ as a function of U for a large value of n when the chemical potential approaches the very narrow peak in the DOS. For n close to 4/3, there is a pronounced maximum at a small value of U, indicating the possibility of a strong enhancement of γ. For n close to 5/3, the enhancement is even larger and is observed for all values of U with a divergence in the $U = 0$ limit.
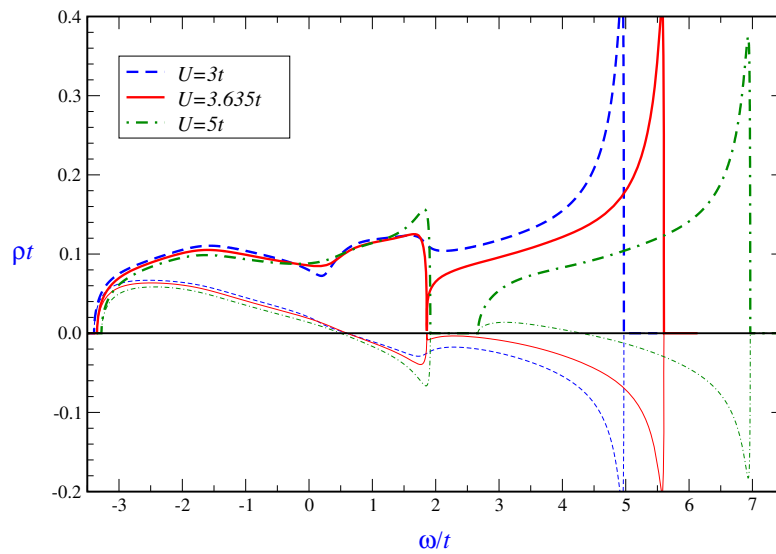
Figure 1. Densities of states $\rho(\omega)$ and $\rho_{nn}(\omega)$ for $n = 1$ and different values of the correlation U.
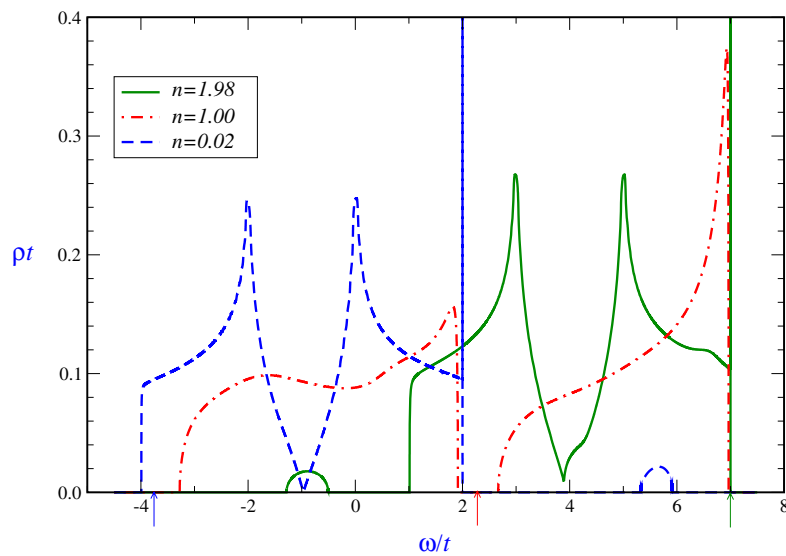

Figure 2. Densities of states for $U = 5t$ and different concentrations n. Arrows indicate the position of the chemical potential.

4. Conclusion

We have studied the effect of the correlation U and band filling n on the DOS and specific heat of the Hubbard model on a kagome lattice. The adopted CPA approximation is the simplest decoupling which provides a qualitatively correct description of the MIT. The renormalization of the self-energy is taken into account via equation (7) and it is fundamental for yielding the correct weights of the Hubbard bands when asymmetric DOS are involved. Away from
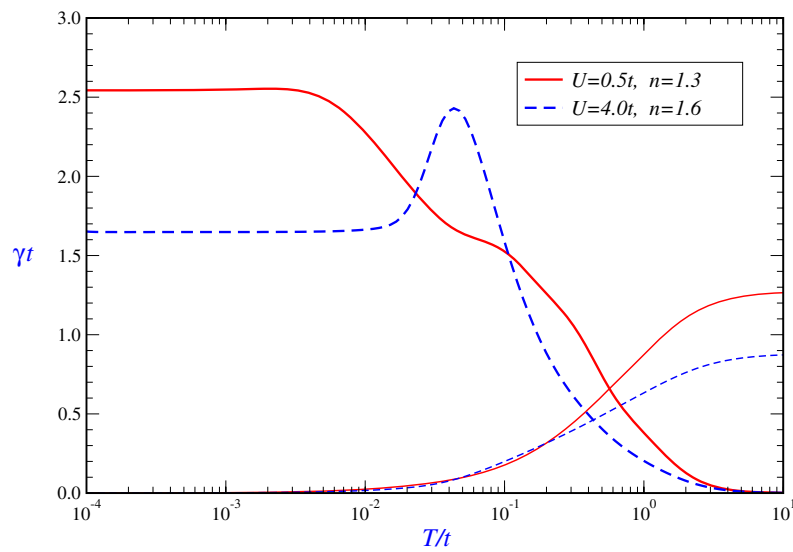
Figure 3. Coefficient γ as a function of temperature for fixed n and U. Thin lines are the integrated entropy.
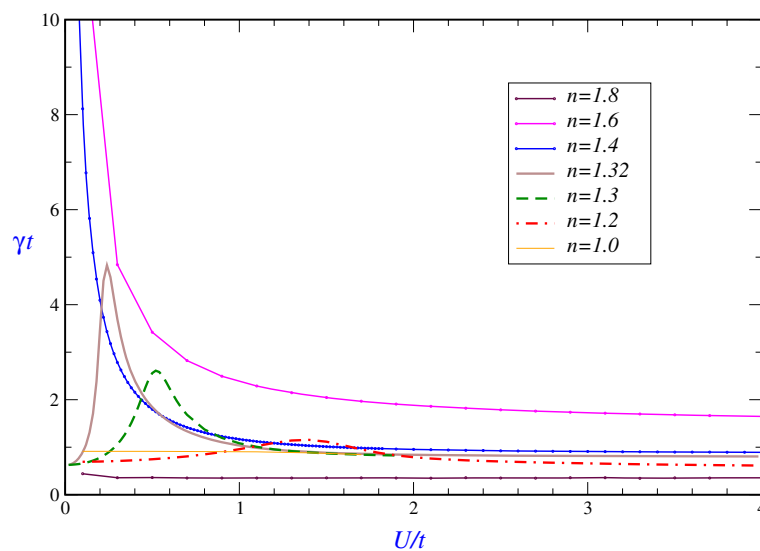

Figure 4. Coefficient γ as a function of U for several concentrations n in the low temperature limit.

half-filling, the CPA takes into account the transfer of spectral weight between the Hubbard bands, interpolating properly between the empty and full band limits. A nearly flat band is present at the top of the band structure, originating from the completely flat band in the uncorrelated DOS of the kagome lattice. For concentrations $n > 4/3$, the chemical potential may be located in this very narrow band, and depending on the value of U, one obtains a significant enhancement of the γ coefficient of the specific heat. Projecting this result to the pyrochlore lattice, which exhibits a doubly degenerate flat band, a similar situation could be

5

found for moderate values of n, in correspondence to what is found in real compounds. In order to describe LiV_2O_4, the model should be extended to include degenerate 3d bands.

Acknowledgment

References

[1] Stewart R (ed) 2004 *Proc. Highly Frustrated Magnetism 2003 Conf.*; *J. Phys.: Condens. Matter* **16** S553–922
[2] Ballou R, Lelivre-Berna E and Fak B 1996 *Phys. Rev. Lett.* **76** 2125
[3] Kondo S *et al* 1997 *Phys. Rev. Lett.* **78** 3729
[4] Urano C *et al* 2000 *Phys. Rev. Lett.* **85** 1052
[5] Anisimov V I *et al* 1999 *Phys. Rev. Lett.* **83** 364
[6] Takada K *et al* 2003 *Nature* **422** 53
[7] Yonezawa S *et al* 2004 *J. Phys. Condens. Matter* **16** L9
[8] Yanagishima D and Maeno Y 2001 *J. Phys. Soc. Japan* **70** 2880
[9] Katsufuji T, Hwang H Y and Cheong S-W 2000 *Phys. Rev. Lett.* **84** 1998
[10] Isoda M and Mori S 2000 *J. Phys. Soc. Japan* **69** 1509
[11] Tsunetsugu H 2002 *J. Phys. Soc. Japan* **71** 1844
[12] Yamashita Y and Ueda K 2003 *Phys. Rev.* B **67** 195107
[13] Imai Y, Kawakami N and Tsunetsugu H 2003 *Phys. Rev.* B **68** 195103
[14] Bulut N, Koshibae W and Maekawa S 2005 *Phys. Rev. Lett.* **95** 037001
[15] Gebhard F 1997 *The Mott Metal–Insulator Transition* (Berlin: Springer)